Universal Journal of Lasers, Optics, Photonics & Sensors
UINUJLOPS004/ Erlin He

ETEXT

Well Optimized Linear Finder (WOLF) Atmospheric Turbulence Compensation (ATC) computational speed improvement through the adoption of parallel, pre-calculated constant complex exponential phase difference chains.

Erlin He, William Arrasmith, PhD and Yang Xin
Florida Institute of Technology, Department of Computer Engineering and Sciences,
150 W. University Blvd. Melbourne FL 32901
ehe2011@my.fit.edu , warrasmi@fit.edu, and yxin2012@my.fit.edu

Received: 8 June 2021; **Accepted:** 18 June 2021; **Published:** 29 June 2021

Citation: Erlin He, William Arrasmith, PhD and Yang Xin Well Optimized Linear Finder (WOLF) Atmospheric Turbulence Compensation (ATC) computational speed improvement through the adoption of parallel, pre-calculated constant complex exponential phase difference chains: 21-30.

The Well-Optimized Linear Finder (WOLF) high-speed, phase-dominant, transfer function estimation method, developed by Professor William W. Arrasmith at Florida Institute of Technology, is a novel, high-speed, transfer function estimation method that, among other things, can be applied to atmospheric turbulence compensation (ATC)/blind deconvolution optical imaging problems. The WOLF methodology uses a diversity-based approach and an adapted error metric to quickly remove the effects of atmospheric turbulence and system noise effects that are present in an incoherent, optical imaging system. In our research, we improve the performance of the WOLF algorithm by investigating the impact of applying parallel processing technology to pre-calculate an expanding set of constant complex exponential phase difference sums that lie at the core of the WOLF methodology. Depending on the number of entrance pupil plane sample points in the image, these complex exponential phase differences can range from an initial single complex exponential phase difference term to sums of millions of complex exponential phase difference terms. We use order analysis on the WOLF algorithm to evaluate the theoretical implications of pre-calculating the constant exponential phase difference chain terms in parallel, and in advance, of when they are needed. We validate the theoretical predictions by using computer simulations to isolate the timing associated with the determination of the constant complex exponential phase difference terms and show that a conservative estimate of approximately 88.7 percent faster performance can be achieved by just implementing the pre-calculation of the sums of constant complex exponential phase difference terms themselves. A representative 256 x 256-pixel image was used in our analysis and computer simulation. The computer used in the study was an un-modified 2014 MacBook Pro computer with a 2.8 GHz (Quad-Core, Intel Core i7) with 16 GB of 1600 MHz DDR3 memory, and a NVIDIA GeForce GT 750M 2 GB video card running Matlab 2020b. Removing the atmospheric turbulence from the 256 x 256 image took approximately 8.2 seconds with the non-optimized WOLF algorithm without taking advantage of parallel processing, or the pre-calculation of the constant complex exponential phase difference terms.

ETEXT

INTRODUCTION

In the field of image processing, many factors contribute to the loss of spatial resolution of a detected image but the atmospheric turbulence is the dominant factor in many well-designed imaging systems [1-6]. One technique which has the goal to restore high-resolution images in the presence of phase aberrations is the method of phase diversity, first proposed by Gonsalves [7]. The phase diversity atmospheric turbulence compensation (ATC) technique is a well-known method which provides an approach for overcoming the effects of atmospheric turbulence and instrument related aberrations by using pairs of images obtained from the same object with relative known phase differences [8-13]. Practically, one of these images is the conventional image that has been degraded by some unknown aberrations and a second image of the same object is obtained by perturbing the unknown aberrations in a known way at the points within the entrance pupil plane aperture. The image collected in a second optical channel contains the effects of the unknown aberrations but will also be influenced by the diversity operation (e.g., adding defocus), which adds a known phase to the conventional image so that the estimate for the object and the unknown aberrations can be made from these two images, and a suitable error metric.

The phase diversity technique provides a well-known conventional method for overcoming the effects of atmospheric turbulence. However, the phase diversity method is computationally intensive, has too many iterations, and needs hours to days to correctly provide the Optical Transfer Function (OTF) estimate. A new high-speed diversity-based imaging method for parallel atmospheric turbulence compensation was recently developed. In the next section, we will briefly introduce the traditional ATC method, and the new WOLF methodology [14], and present an approach to improve the performance of the WOLF algorithm. We also make a performance assessment through computer simulation to estimate the effects of our improvement.

ANALYSIS

In this section, we review a thoroughly documented traditional diversity-based ATC method. The well-known phase diversity technique requires a pair of images which provide a known diversity through the simultaneous capture of two related images (e.g., de-focus and in-focus images) that freeze the state of the atmosphere. A suitable error metric such as the Gonsalvez error metric, can be used to estimate the OTFs for the de-focus and in-focus images. The Gonsalvez error metric is given by,

$$E(\vec{f}) = \frac{\left|I(\vec{f})\hat{H}_d(\vec{f}) + I_d(\vec{f})\hat{H}(\vec{f})\right|^2}{\left|\hat{H}(\vec{f})\right|^2 + \left|\hat{H}_d(\vec{f})\right|^2} \quad (1)$$

where $I(\vec{f})$ and $I_d(\vec{f})$ are the image spectra for the paired images, $\hat{H}(\vec{f})$ and $\hat{H}_d(\vec{f})$ are the estimates of the optical transfer function for the paired images (the "^" symbol represents an estimated value). In traditional diversity-based atmospheric turbulence compensation methods, the process for estimating the OTF and diversity OTF is:

1. Use the Zernike polynomials to initialize an entrance pupil plane phase estimate $\theta(\vec{x})$. This is usually an initial state of weighted Zernike basis functions.
2. Use an initial guess of the entrance pupil phase $\theta(\vec{x})$, to form the generalized pupil function (GPF), $w(\vec{x})$, by using Equation (2),

$$w(\vec{x}) = A\,(\vec{x})e^{j\theta(\vec{x})}. \quad (2)$$

ETEXT

Note: use $w_{pd}(\vec{x}) = A\,(\vec{x})e^{j(\theta(\vec{x})+\theta_{pd}(\vec{x}))}$ for estimating the diversity GPF. $A\,(\vec{x})$ is an amplitude function that is one inside the clear aperture of the imaging system and zero outside. The value $\theta_{pd}(\vec{x})$ is the known phase diversity term that is added beforehand (e.g., defocus).

3. Zero-pack the GPF for sampling reasons in preparation of generating an OTF estimate.
4. Form the impulse response in accordance with Equation (3),

$$h_i(\vec{x}) = \mathcal{F}^{-1}(\,w(\vec{x}))\,. \tag{3}$$

5. Determine the point spread function (PSF) estimate $|h_i(\vec{x})|^2$ by pointwise taking the magnitude squared of the result of the impulse response from the previous step.
6. Obtain the OTF estimate by using Equation (4),

$$\hat{H}(\vec{f}) = \frac{\mathcal{F}(|h_i(\vec{x})|^2)}{\mathcal{F}(|h_i(\vec{x})|^2)_{\vec{f}=0}}\,. \tag{4}$$

7. Since both the OTF and diversity OTF estimates can be formed by using $w(\vec{x})$ and $w_{pd}(\vec{x})$ in this process, we can determine the error at each spatial location in the OTF by substituting the result from Equation (4) into the Gonsalvez error metric given in Equation (1).
8. Find the best OTF estimate by minimizing the Gonsalvez error metric and keeping the OTF associated with the minimum error value. Figure 1 illustrates these processes.

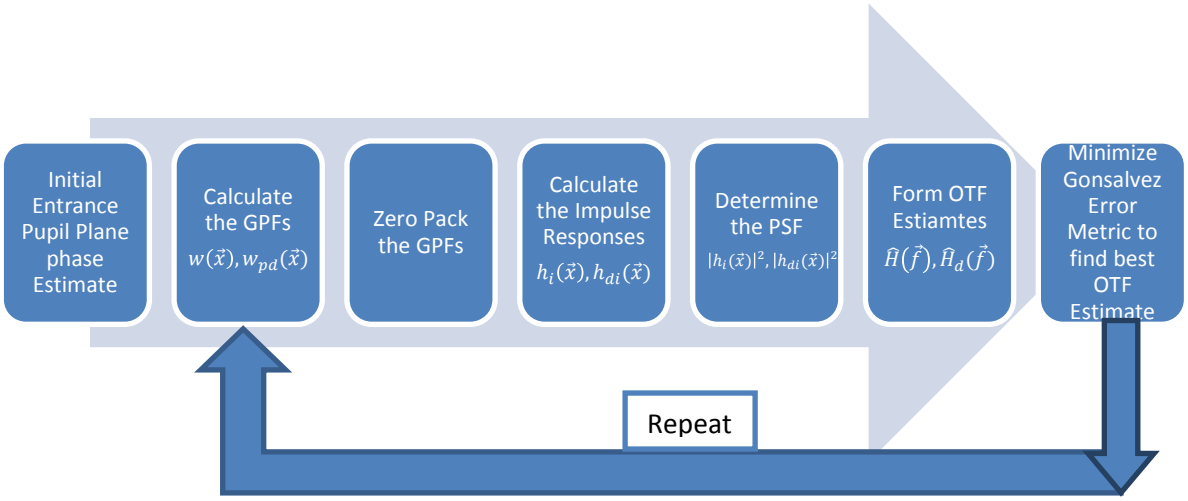

Figure 1 Traditional ATC Method Functional Flow Block Diagram to estimate OTF.

The following process is used to minimize the Gonsalves error metric.

1. Determine the total summed error by adding all the errors obtained from the initial entrance pupil plane phase estimation errors, shown in Step 7 above.
2. Adjust the weights on the Zernike polynomials to come up with a new entrance pupil plane phase estimate.
3. Generate a new error estimate by repeating the previous steps 2 through 8.
4. Compare the new error estimate to the old estimate and keep the phase estimates associated with the lowest error.
5. Continue to execute steps 3 and 4 until the error is minimized and the best OTF and diversity OTF estimates are obtained.

To summarize the traditional phase diversity ATC process, we form the OTF estimate by first determining the weights on the Zernike polynomials and initialize the entrance pupil plane phase estimate to form the generalized pupil function phase. We then calculate the OTFs and diversity OTFs as a function of the Zernikes by determining the PSF. To estimate the best OTF, some optimization methods may need to be applied to minimize the error metric. By the end of the process, we will obtain the best estimate of the OTF and the diversity OTF. After the best OTF estimate is determined, the inverse of $\hat{H}(\vec{f})$ can be used to determine the ATC filter function,

$$H^{-1}(\vec{f}) = \frac{H^*(\vec{f})}{(|H(\vec{f})|^2 + \alpha)}. \quad (5)$$

Here α is a standard regularization parameter for the case when $|H(\vec{f})|^2$ is close to zero. By multiplying both sides of $I(\vec{f}) = O(\vec{f})H(\vec{f})$ by this filter function, we get,

$$O(\vec{f}) = I(\vec{f})H^{-1}(\vec{f}). \quad (6)$$

In the final step, the atmospheric turbulence free object brightness estimate can be found by a 2-D inverse Fast Fourier Transform (IFFT) of Equation (6).

We now present an overview of the WOLF methodology. To produce an accurate OTF estimate, the WOLF paradigm derives the OTF by using the conventional normalized spatial autocorrelation of the generalized pupil function (GPF),

$$\mathcal{H}(\vec{f}) = \frac{W(\vec{x}) \otimes W(\vec{x})}{W(\vec{0}) \otimes W(\vec{0})}, \quad (7)$$

where the symbol $\otimes$ represents the autocorrelation process. Note that the diversity OTF can be similarly determined by replacing $W(\vec{x})$ by $W_{pd}(\vec{x})$ in Equation (7). It is helpful to use a visual representation of the numerator of Equation (7) to understand the advantages of the WOLF paradigm. The denominator of Equation (7) is just a scaling factor equal to the total number of non-zero sample points in the entrance pupil plane.

The above autocorrelation equation makes every point of the OTF a function of summations of complex exponential phase differences. Note that the amplitude term $A(\vec{x})$ is set to one for near-field atmospheric turbulence applications such as Earth-to-air, or Earth-to-space imaging systems. Instead of modeling the entrance pupil plane phase by using the Zernike basis functions as in traditional phase diversity ATC methods, the WOLF method directly determines the entrance pupil plane phases through an intelligent combination of phase difference result. This approach takes advantage of redundancies in the OTF phases and inherent symmetries in the OTF. We now present some insights into the special way to determine the autocorrelation of the GPF and stitch together the results.

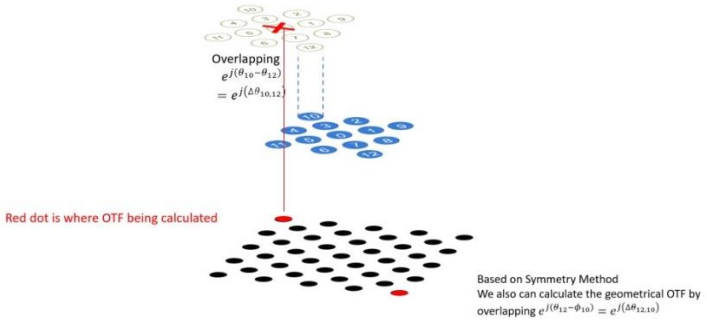

Figure 2 Complex exponential phase differences (and conjugates) for the one-point overlap case.

In Figure 2, the blue dots represent a fixed array of the entrance pupil plane phase on a representative 13-point triangular aperture. The green circles represent a moving array that consists of a copy of the original blue phases but is vertically and horizontally translated with respect to the blue array. In this case, the green array is translated so that only 1 point overlaps (the so-called one-point overlap scenario). The black dots represent the total points where the OTF is being calculated for all possible overlaps, and the red X represent the point where the OTF is currently being determined. Each point in the OTF can be calculated by placing the center of the moving array of the entrance pupil plane phase (denoted by the red X) on the OTF point in question (denoted by the upper left red dot on the

black array) and overlapping the moving array points with the fixed array. Note that the numbers on the fixed and moving arrays represent the entrance pupil plane phase at the respective array positions. As an example, the overlapping points in Figure 2 are blue (10) and green (12). The manner in which the phases are combined is that the phase at the green coordinate is subtracted from the phase at the blue coordinate. For the case shown in Figure 2, this leads to $\Delta\theta_{10,12} = \theta_{10} - \theta_{12}$. The OTF at the red dot in Figure 2 is then given by $\frac{e^{j\Delta\theta_{10,12}}}{N_{ep}}$, where N_{ep} is the total number of the entrance pupil plane points (in this case 13). Figure 2 represents the one-point overlap case. Notice also that by solving for the OTF at the location of the darker red dot, we simultaneously solve for the OTF value at the lighter red dot across the array through conjugate symmetry. Next, we show the two-point overlap case in Figure 3.

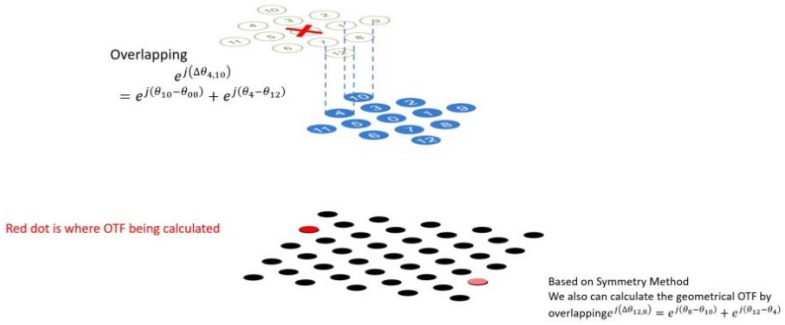

Figure 3 Complex exponential phase differences (and conjugates) for the two-point overlap case.

Notice that we now have 2 points of the blue and green arrays that are overlapping (two-point overlap case) and the two phase differences are again determined by subtracting the green phases at the numbered locations from the respective blue phases. The complex exponentials on the left side of Figure 3 show the unnormalized OTF. By dividing these complex exponentials by N_{ep}, the OTF at the dark red dot can be determined. It is an interesting property of the WOLF methodology that the results of the one-point overlap problem are fed into the two-point problem so that only one phase difference, $\Delta\theta_{r,s}$ is unknown. The WOLF_Iota algorithm solves this phase difference and also the individual phases, θ_r and θ_s for the two-point overlap case.

Below we see the three-point overlap case in Figure 4. As before, the overlapping green phases are pointwise subtracted from the blue phases and they are pointwise raised to respective complex exponentials and normalized as before to determine the OTF. The previous results are fed into WOLF_Rho to determine a complex constant used by WOLF_Alpha. WOLF_Alpha then determines the only two unknown phases. It is an interesting property of the WOLF methodology that for overlaps larger than three points, these can all be reduced to the three-point case with only 2 unknown phases and the combination of WOLF_Rho and WOLF_Alpha can solve for these unknown phases.

ETEXT

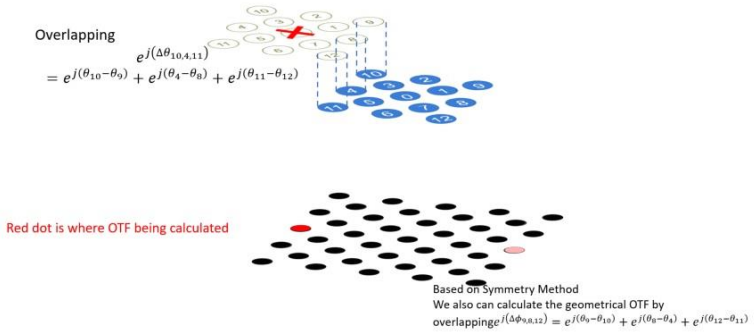

Figure 4 Complex exponential phase differences (and conjugates) for the three-point overlap case.

In Figure 5 we see all the parts of the OTF that need to be calculated to fully determine all the entrance pupil plane phases. This is accomplished by the phase symmetries in the OTF and the specialized phase "stitching" method inherent in the WOLF paradigm. We only need to calculate $\frac{N_{ep}}{2}$ OTF points to uniquely define all the entrance pupil plane phases. With 2 processors, the WOLF method scales as $\frac{N_{ep}}{4}$.

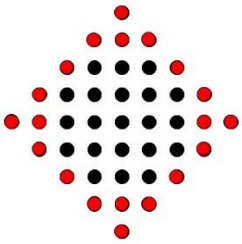

Figure 5 OTF is being calculated (red dots) after three-point overlap.

The WOLF paradigm applies to general linear and linear shift-invariant systems that use a diversity-based imaging approach. The WOLF method can reduce the time complexity of the overall ATC problem. The following Functional Flow Block Diagram (FFBD) in Figure 6 illustrates the internal dynamics and major algorithms in the WOLF methodology.

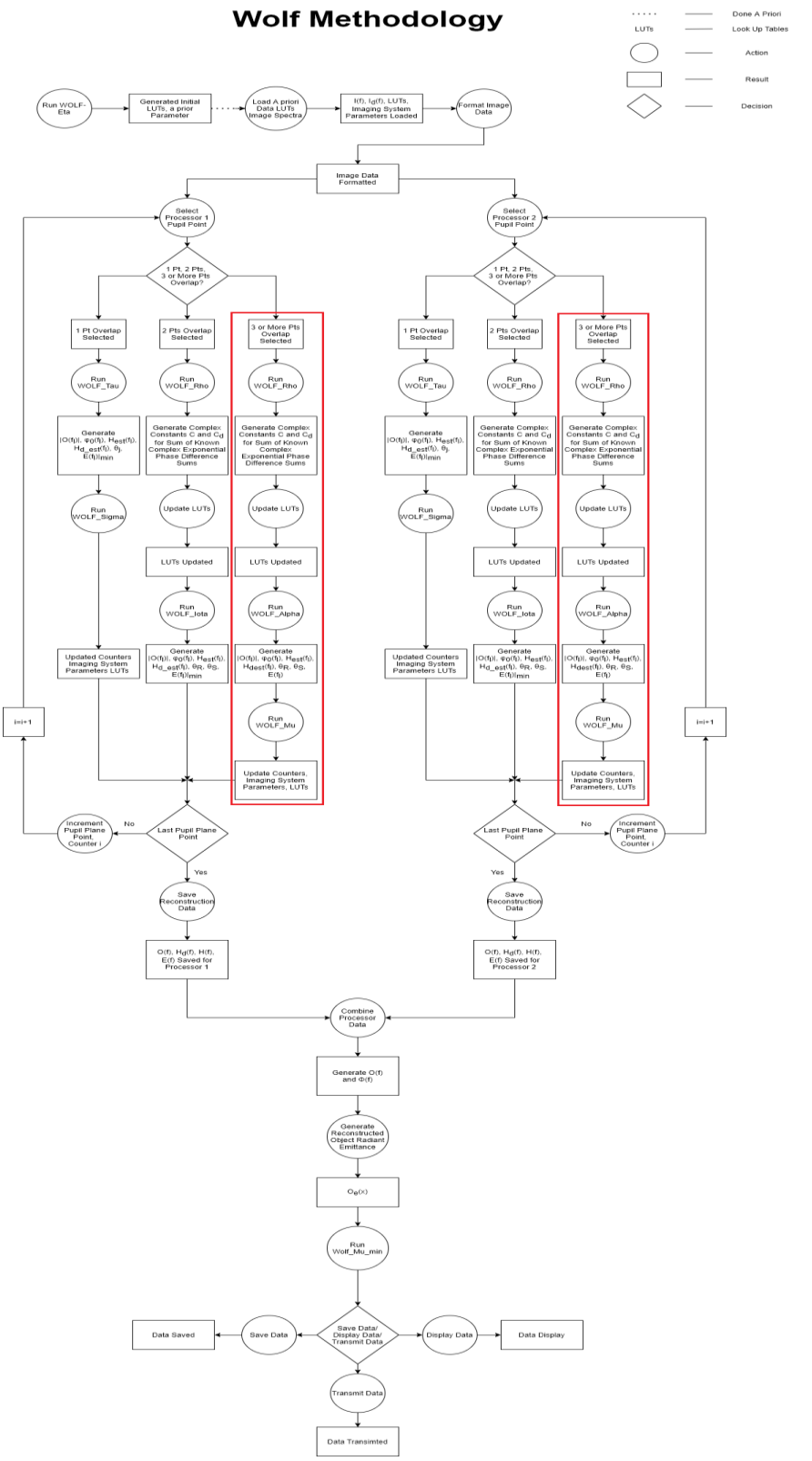

Figure 6 WOLF flow diagram.

ETEXT

Previous time complexity studies [15] showed that the third path in the red box which includes WOLF_Rho, WOLF_ Alpha and WOLF_Mu is the only path that affects the time complexity because this path is executed for every OTF point with more than two overlapping points and so dominates the time complexity analysis. The WOLF_Tau algorithm (one-point overlap) and WOLF Iota (two-point overlap) algorithm only need to be executed twice and four times respectively and so do not substantially contribute to the time complexity and can be safely ignored for entrance pupils with sufficiently large number of sample points N_{ep}. The WOLF_Rho algorithm generates the complex constants C and Cd that sums the known complex exponential phase differences that have been previously determined by the WOLF method and that are needed by the main WOLF_Alpha algorithm that determines the unknown entrance pupil plane phases, and the OTF and diversity OTF estimates. WOLF_Mu currently has diagnostic information and updates internal counters, and its execution time should be negligible when compared to WOLF_Rho and WOLF_Alpha. In this work, we improve the computational performance of the WOLF algorithm by applying parallel processing techniques to pre-calculate the expanding set of constant complex exponential phase difference sums that result from the increasing phase overlaps. Next, we present how the pre-calculation of the constants works in the WOLF_Rho algorithm by illustrating the three-point overlap case as shown in Figure 4 as an example.

As seen in Figure 4, the un-normalized OTF can be represented as a sum of complex exponential phase differences, $e^{j(\Delta\theta_{i,s}^{\lambda_1})} + e^{j(\Delta\theta_{m,n}^{\lambda_1})} + e^{j(\Delta\theta_{r,j}^{\lambda_1})}$, and we know $\theta_i^{\lambda_1}$ and $\theta_j^{\lambda_1}$ from the one-point overlap process. We also know $\theta_m^{\lambda_1}$ and $\theta_n^{\lambda_1}$ from the two-point overlap process. The only phase differences we need to determine during the three-point overlap are $\Delta\theta_{i,s}^{\lambda_1}$ and $\Delta\theta_{r,j}^{\lambda_1}$ by solving for $\theta_s^{\lambda_1}$ and $\theta_r^{\lambda_1}$with the WOLF_Alpha algorithm. The constant for this three-point overlap can be calculated by using the WOLF_Rho algorithm. The same logic follows in that, after we finish the calculation of the constants from the three-point overlap, we can pass this result to the four-point overlap case and to all subsequent overlap cases. In effect WOLF_Rho sums a series of known complex exponential phase differences. This can be thought of as a "chain" of complex exponential phase differences that are summed together.

To explain this complex exponential phase difference chain mathematically, we define the entrance pupil as an MxN matrix, y' and x' represent the number of points which overlap at any given moment in the y direction and x direction respectively, k' and k represents the counter number during the overlapping process and both k' and k should range from 1 (one-point overlap) to the maximum number of y' and x'. Therefore, the equation for the sum of entrance pupil plane complex exponential phase differences (the constants calculated from WOLF_Rho) at wavelength $\lambda_1$for a given x'y' - 2 overlapping points can be described as,

$$C_{est} = \sum_{k'=1}^{\mathrm{y}'} \sum_{k=1}^{\mathrm{x}'} e^{1i(\theta_{k',k}^{\lambda_1} - \theta_{M-\mathrm{y}'+k',\ N-\mathrm{x}'+k}^{\lambda_1})} \tag{8}$$

The factor of 2 in the number of overlapping points stems from the first and last overlapping points containing the unknowns that are calculated by WOLF_Alpha. These points are removed from the calculation of the constant C_{est} and are determined by WOLF_Alpha. Depending on the number of entrance pupil plane sample points, these complex exponential phase differences can range from an initial single complex exponential phase difference term (one-point overlap) to sums of millions of complex exponential phase difference terms for large numbers of overlapping points (x' and y' are large). Therefore, the time complexity of the calculation for Equation (8) could be very significant if we do not pre-calculate Equation (8) where possible. By pre-calculating the constant in Equation (8), we can reduce the computational time to just 3 complex exponential sums instead of potentially millions of complex exponential phase differences. This substantially reduces the time to calculate WOLF_Rho. We use order analysis on the WOLF methodology to evaluate the theoretical implications of pre-calculating the constant complex exponential phase difference chain terms in parallel, and in advance, of where they are currently needed.

We present the results of our order analysis in the next section and assess our results using computer simulation.

ETEXT

RESULTS

The primary WOLF algorithms on the critical path for time complexity analysis are WOLF_Rho, WOLF_Alpha, and WOLF_Mu as seen in Figure 6. In this section we present the results of an order analysis on pre-calculating the constants determined by WOLF_Rho. We also validate this analysis using computer simulation. For the final version of the WOLF algorithm, WOLF_Mu can be ignored since it will only reset some internal indices. We include it for now. We now evaluate the impact of pre-calculating the constant C_{est} on an example. As mentioned previously, WOLF_Alpha is the primary algorithm that calculates the needed phase and OTF products for the case of 3 or more overlapping points. A representative 256 x 256-pixel image was used in our analysis and computer simulation. The computer used in the study was an un-modified 2014 MacBook Pro computer with a 2.8 GHz (Quad-Core, Intel Core i7) with 16 GB of 1600 MHz DDR3 memory, and a NVIDIA GeForce GT 750M 2 GB video card running Matlab 2020b. Removing the atmospheric turbulence from the 256 x 256 image took approximately 8.2 seconds with the non-optimized WOLF algorithm without taking advantage of parallel processing, or pre-calculating the constant terms of WOLF_Rho according to Equation (8). Figure 7 shows the before and after results of the aberrated and corrected images.

Figure 7 Aberrated image with Gaussian noise (left) and corrected image by using the WOLF method (right).

To improve the computational speed of the WOLF algorithm, we can pre-calculate the majority of the calculations in WOLF_Rho according to Equation (8). We conducted timing studies of the critical algorithms in the time complexity study of the WOLF paradigm. We found the approximate execution time for WOLF_Rho is $2.0446 \times 10^{-4}s$, WOLF_Alpha is $1.3013 \times 10^{-4}s$, and WOLF_Mu is $8.1106 \times 10^{-4}s$. This gives a theoretical expected execution time of 9.2 seconds for our time complexity analysis. This matches our actual simulated results of 8.2 seconds for the case shown in Figure 7 very well and our simulated result falls within one standard deviation of our theoretical results. By pre-calculating Equation (8) and optimizing WOLF_Mu, the expected execution time becomes 1.04 seconds for the improved WOLF algorithm, an improvement of 88.7 percent over the current version. Future parallel implementations are expected to improve the processing speed by several orders of magnitude.

CONCLUSION

A novel, high-speed, diversity-based transfer function estimation method, the Well Optimized Linear Finder (WOLF) paradigm, that can be applied to atmospheric turbulence compensation and blind deconvolution optical imaging problems, was briefly summarized. A time complexity study was done to show that pre-calculating

ETEXT

determined complex exponential phase difference sums can substantially improve the computational speed of the WOLF algorithm. The time complexity analysis determined approximately 9.2 seconds expected execution time for a 256 by 256 pixel image. This theoretical time was compared to a computer simulated 256 by 256-pixel image correction which took an actual 8.2 seconds, a remarkably good comparative result considering that the simulated result fell within one standard deviation of our theoretical results. By pre-calculating the WOLF_Rho calculations shown in Equation (8), the execution time is expected to be 1.04 seconds. This is an 88.7 percent improvement over the current implementation of the WOLF method. In future efforts, we plan to investigate some parallel processing improvements to the WOLF methodology that have the potential of increasing the processing speed by several orders of magnitude making real-time ATC with the WOLF methodology highly practicable.

REFERENCES

1. R. G. Paxman and J. R. Fienup, "Optical misalignment sensing and image reconstruction using phase diversity," *J. Opt. Soc. Am.*, Vol. 5, No. 6, p914-923, 1988.
2. R. G. Paxman, J. H. Seldin, M. G. Loefdahl, G. B. Schmarmer, and C. U. Keller, "Evaluation of Phase-Diversity Techniques for Solar Image Restoration," *J. Astrophysical*, Vol. 466. P1087, 1996.
3. M. C. Roggemann, B. Welsh: *Imaging through Turbulence*, CRC Press, New York, 1996.
4. Michael C. Roggemann, and Byron Welsh, *Imaging through Turbulence*, CRC Press (1996)
5. R. J. Noll, "Zernike Polynomials and atmospheric turbulence," *J. Opt. Soc. Am.*, Vol. 66, pp. 207-211, 1976.
6. Glenn A. Tyler "Adaptive optics compensation for propagation through deep turbulence: a study of some interesting approaches," *Optical Engineering* 52(2), 021011 (15 November 2012)
7. R. A. Gonsalves and R. Chidlaw, "Wavefront Sensing by Phase Retrieval," *Proc. On Applications of Digital Image Processing III*, SPIE, Vol. 207, 1979.
8. R. A. Gonsalvez, "Phase Retrieval and Diversity in Adaptive Optics," J. of Optical Engineering, Vol. 21, Num. 5, 1982.
9. R. A. Gonsalves, "Phase Techniques for imaging and Recognition", RADC-TR-90-61, Final Technical Report, May 1990.
10. R. A. Gonsalves, "Phase diversity: math, methods, and prospects, including sequential diversity imaging," Proc. SPIE 10677, Unconventional Optical Imaging, 106771S (24 May 2018).
11. R. G. Paxman, T. J. Schulz, and J. R. Fienup, "Joint estimation of object and aberrations by using phase diversity," *JOSA A 9*, p1072–1085, 1992.
12. Laurent M. Mugnier, Amandine Blanc, Jérôme Idier, "Phase Diversity: A Technique for Wave-Front Sensing and for Diffraction-Limited Imaging,"*Advances in Imaging and Electron Physics*, Elsevier,Volume 141,2006,
13. David A. Carrara, Brian J. Thelen, and Richard G. Paxman "Aberration correction of segmented-aperture telescopes by using phase diversity", Proc. SPIE 4123, Image Reconstruction from Incomplete Data, (16 November 2000).
14. W. W. Arrasmith, "HIGH-SPEED DIVERSITY-BASED IMAGING METHOD FOR PARALLEL ATMOSPHERIC TURBULENCE COMPENSATION," U.S. patent number: US 8,447,129 B2, May 21, 2013.
15. Y. Xin, "Order Analysis Comparison between traditional Fourier Transform-based atmospheric turbulence compensation methods and new Well Optimized Linear Finder Methodology", International Scientific Conference on Lasers, Optics, Photonics and Sensors, June 2021.